scatter, while the smallest impactors are systematically higher. The departures for hypervelocity data are increased when equation (10*d*) is applied (Figure 5, bottom) but accommodates small projectile data at low velocities. The difference between low and high velocity impact data could reflect a contributing role of cohesion. From analysis by *Schmidt and Holsapple* [1980], cohesion effects would be expressed by a lower than expected value of $k\pi_2{}^{\alpha}\pi_v$ at higher impact velocities. Under vacuum conditions, however, higher impact velocities do not result in comparable reduction. The presence of even a 0.03-bar atmosphere significantly reduces cratering efficiency to 20% and 35% the expected value for pumice and sand, respectively, referenced to vacuum conditions.

Application of equation (10*d*) to the microsphere, coarse sand, and sand-mixture targets is shown in Figure 6 with no. 140-200 and pumice shown for reference. As might be expected from Figure 3*a*, the effects of an atmosphere on

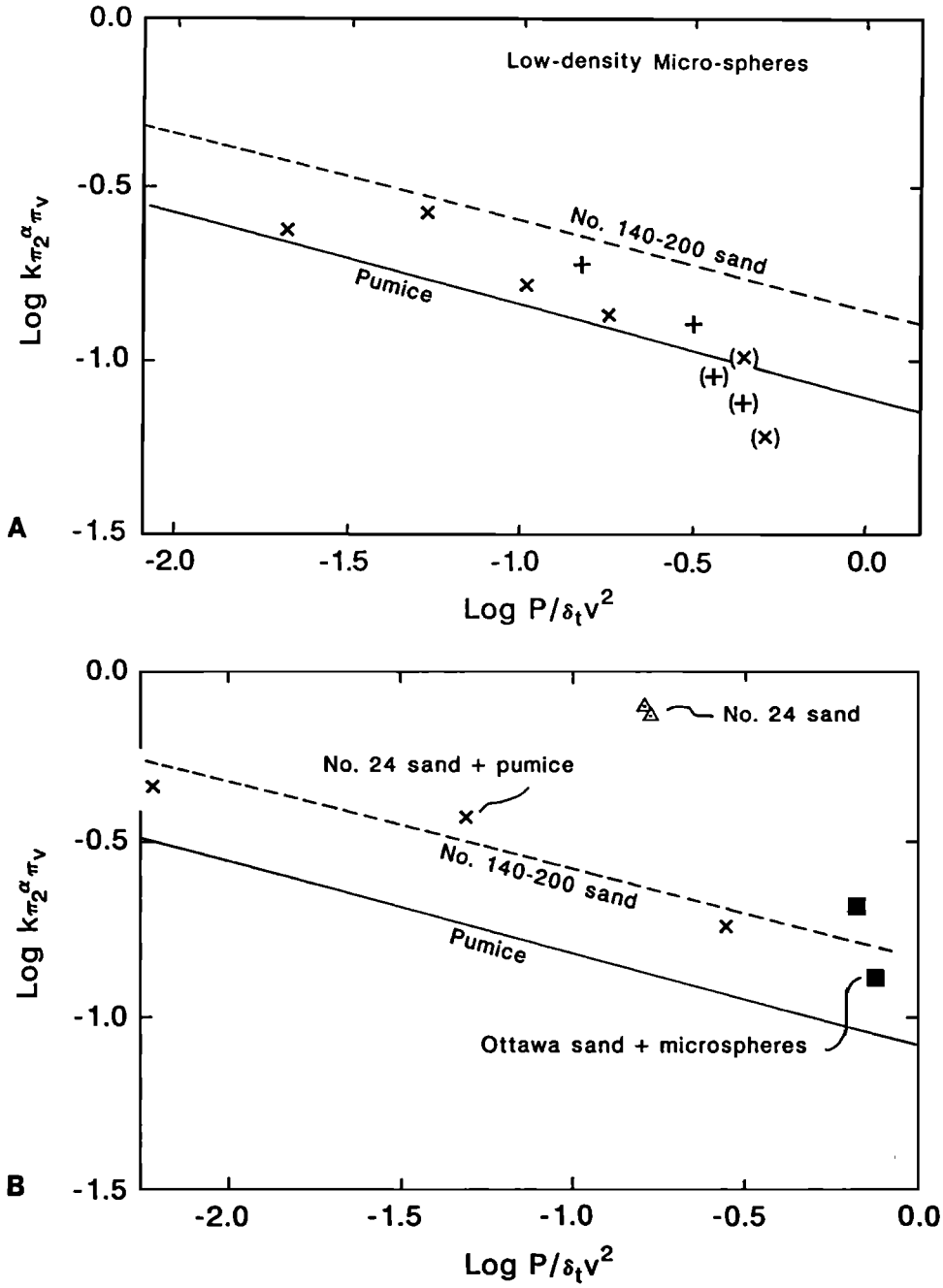

Fig. 6. (*a*) Reduction in cratering efficiency as a function of the dimensionless pressure scaling parameter given by equation (10*c*) for impacts into a target of low-density microspheres. Although the internal angle of friction for target of microspheres (20°) is significantly less than both sand (30°) and pumice (80°), the observed response is similar. Parentheses indicate experiments where rim collapse was observed to occur immediately following formation. Pressure is in bars; velocity is in kilometers per second. (*b*) The effect of an atmosphere on cratering efficiency for coarse sand targets and targets mixed with a small component of fine-grained material. Introduction of only 8% pumice by weight to no. 24 sand or 5% microspheres to Ottawa sand dramatically reduces cratering efficiency. Introduction of either fine-grained fraction to the sand produced no observable effect on the internal angle of friction. Pressure is in bars; velocity is in kilometers per second.